Comparative genomics reveals multipartite genomes undergoing loss in the fungal endosymbiotic genus *Mycetohabitans*

Bhuwan Abbot[1], Sara Field[1], Lauren Carneal[1], Richard Allen White III[2,3], Andra Buchan[2], Caroline West[2], Laira Lee[4], Morgan Elizabeth Carter[1,3]

1. Department of Biological Sciences, The University of North Carolina at Charlotte, Charlotte, NC, 28223, USA
2. Department of Bioinformatics and Genomics, The University of North Carolina at Charlotte, Charlotte, NC, 28223, USA
3. CIPHER Center, The University of North Carolina at Charlotte, Charlotte, NC, 28223, USA
4. North Carolina School of Science and Mathematics – Morganton, Morganton, NC, 28655, USA

Corresponding Author Email: morgan.carter@charlotte.edu

ABSTRACT

Endosymbiotic bacteria extensively impact phenotypes of their eukaryotic hosts, while experiencing dramatic changes to their own genome as they become more host-restricted in lifestyle. Understanding the trajectory of such a genome has largely been done through study of animal-associated bacteria, especially insect endosymbionts. Yet, endofungal bacteria provide another natural experimental model for investigating how microbial genomes change when living inside of a host cell. *Mycetohabitans* spp. are culturable bacterial endosymbionts of the Mucoromycota fungus *Rhizopus microsporus*. To investigate the genome dynamics resulting from the endohyphal nature of this emerging model genus, we long-read sequenced and assembled new complete genomes to combine with previous assemblies, creating a global dataset of 28 complete *Mycetohabitans* genomes. All genomes were between 3.3 and 3.9 Mbp in size and were multipartite, structured into two conserved replicons with some strains having an additional plasmid. Based on evolutionary rate and gene content analysis of the different replicons, we termed the two major ones a chromosome and chromid. The differential presence of a third, mobilome-rich plasmid in some strains and the proliferation of transposable elements provide putative mechanisms for recombination or gene loss. The conservation of intact prophage and putative toxin-antitoxin systems, and extensive enrichment of secondary metabolite clusters in the *Mycetohabitans* genomes highlight the dynamic nature of this reducing genome. With fungal-bacterial symbioses becoming increasingly apparent phenomena, lessons learned from this symbiosis will inform our understanding of bacterial adaptation to novel hosts, and the process of microbe-microbe coevolution.

INTRODUCTION

With the increasing ease of bacterial genome sequencing and metagenomics, genetic information on both culturable and unculturable microbes is becoming readily available. Consequently, bacterial evolution is now better understood to be a function of the organism's lifestyle and environment, spotlighting endosymbiotic bacteria as particularly interesting cases to gain insight into genomic changes during coevolution (Keeling and McCutcheon 2017; Wernegreen 2015). It is widely understood through studies of insect symbionts, like the well-studied *Wolbachia* genus, that bacteria with obligate host relationships typically have undergone genome reduction, widespread gene loss, and rapid genome evolution as a result of AT richness (Porter and Sullivan 2023; Vancaester and Blaxter 2023; Wernegreen 2015).

Yet, obligate endosymbionts only represent the segment in this evolutionary journey with high host dependence, and their intractability *in vitro* poses difficulties for investigating processes leading to such a reduced genome. In contrast, genomes belonging to diatom endosymbionts in a transitionary state have expanded and accumulated transposable elements (TEs) and pseudogenes, compared to those in a more stable endosymbiosis that have undergone the expected TE and core gene loss (Grujcic et al. 2025). Similarly, insect endosymbionts with larger genomes like those in the *Sodalis* genus have high pseudogenization (Boyd et al. 2024). Clearly, studying genetic features in intracellular bacteria that are recently host-restricted is needed to reach broad conclusions about genomic evolution during the course of endosymbiosis.

Furthermore, diverse eukaryotes undergo bacterial colonization, from unicellular protists to multicellular organisms like animals, yielding symbiotic outcomes ranging from pathogenic to mutualistic. For example, a wide range of fungi are hosts to endosymbiotic bacteria varying in the permanence and co-dependence within relationships (Pawlowska 2024; Robinson et al. 2021). Arbuscular mycorrhizal fungi (phylum: Glomeromycotina) are extensively found to have obligate relationships with endohyphal bacteria with highly reduced genomes, indicating a fairly ancient relationship (Naumann et al. 2010). Multiple Ascomycetes and Basidiomycetes relevant to plant and human health have facultative bacterial endosymbionts impacting fungal phenotypes and environmental function, such as pathogenesis and metabolism (Moses and Carter 2025; Steffan et al. 2020). However, not much is known about the mechanistic basis of bacterial adaptation to fungal hosts and few genomic studies have been undertaken for this niche (Amses et al. 2023). Hence, fungal-bacterial endosymbioses represent a subfield with a wealth of untapped knowledge for new perspectives on genomic dynamics during bacterial evolution towards an endosymbiotic lifestyle.

A valuable emerging model for fungal-bacterial endosymbiosis is the interaction between the Mucoromycota fungus *Rhizopus microsporus* (Rm) and *Mycetohabitans* spp. (Betaproteobacteria). Rm commonly occurs as cosmopolitan mold and is an opportunistic human and plant pathogen with a global distribution. While not all Rm isolates harbor

Mycetohabitans spp., the ones that do are dependent on their endosymbiont for fungal sporulation and are only capable of vegetive growth when cured (Mondo et al. 2017; Partida-Martinez et al. 2007). Initial studies found that Rm harboring *M. rhizoxinica* (Mrh) causes rice seedling blight, as the bacterium produces the antimitotic toxin rhizoxin needed for pathogenicity (Partida-Martinez and Hertweck 2005; 2007). Many more Rm isolates have since been found to have *M. rhizoxinica, M. endofungorum* (Mef), or unclassified *Mycetohabitans* spp. (Msp) residing within their hyphae (Cabrera-Rangel et al. 2022; Carpenter et al. 2024; Dolatabadi et al. 2016; Lackner et al. 2009). Formerly classified within the genus *Burkholderia*, *Mycetohabitans* spp. have a reduced genome size of about 3 Mbp compared to the 5-8 Mbp observed in free-living Burkholderiaceae, suggesting a specialized symbiosis (Estrada-De Los Santos et al. 2018). However, both partners can be cultured independently and the bacteria horizontally transferred, creating a tractable study system.

Because of their endosymbiotic nature, limited sampling of *Mycetohabitans* isolates and a lack of complete genome assemblies have been obstacles for comparative studies into the structural organization of the endosymbiotic genome and the genetic diversity within this genus. Yet, the symbiosis between Rm and *Mycetohabitans* spp. presents an opportunity to investigate the mechanisms and processes enabling genome loss, and consequently the evolution of an obligate endosymbiotic lifestyle at a transitional period. In this study, we present new complete genome assemblies via long-read sequencing and assess the pangenome of a global collection of 28 complete *Mycetohabitans* genomes. We compare evolutionary dynamics and genome composition of their replicons and investigate the secondary metabolite potential and phage presence within those genomes. Our results show an open pangenome with differential evolutionary stability and conservation across the multipartite genome, revealing the dynamics at play in a facultative-to-obligate transitional endosymbiotic genome.

METHODS

Screening Rhizopus strains for presence of Mycetohabitans

Genomic DNA was extracted from *Rhizopus* spp. grown on Potato Dextrose Agar (PDA) overnight at 28°C using the Quick-DNA Fungal/Bacterial Miniprep Kit (Zymo). PCR using primer sets for bacterial 16S rDNA gene (27F: 5' AGAGTTTGATCTGGCTCAG 3'; 1492R: 5' GGTTACCTTGTTACGACTT 3') was done to confirm bacterial presence (Heuer et al. 1997). Fungal ITS sequence was amplified as a positive control for gDNA quality using the primers ITS86F (5' GTGAATCATCGAATCTTTGAA 3') and ITS4 (5' TCCTCCGCTTATTGATATGC 3') (Turenne et al. 1999) . Standard buffer and protocol for OneTaq 2X Master Mix (New England Biolabs) was used with 30 cycles. Products were visualized using agarose gel electrophoresis.

DNA extraction

Rhizopus spp. were grown on PDA at 28°C until non-sporulating fungal mycelia was visible (2 days). Bacterial extractions were carried out by disrupting hyphal tissue suspended in 10

mM $MgCl_2$ using a bead beater, micropestle, or vortex. Bacteria were separated from fungal hyphae by syringe filtration through 2-2.7 µm filters and plated on King's medium B or lysogeny broth amended with 1% glycerol, each prepared with 1% agar and 100 µg/mL cycloheximide. After incubation at 28°C until colonies were visible, *Mycetohabitans* spp. colonies were inoculated in LB with 1% glycerol or KB broth at 28°C for 3 days. DNA extractions were done using the Wizard® Genomic DNA Purification Kit (Promega) following the protocol for gram-negative bacteria, from turbid bacterial cultures.

Genome sequencing and assembly

The quantity of genomic DNA was assessed using a QubitFlex and sequenced by Plasmidsaurus Inc. using Oxford Nanopore Technology. Library preparation was carried out using v14 library prep chemistry with minimal fragmentation and the libraries were sequenced using Oxford Nanopore Technologies R10.4.1 PromethION flow cells. Assembly was also carried out by Plasmidsaurus using Filtlong v0.2 (github: rrwick/Filtlong) for eliminating low quality reads and downsampling when necessary, Miniasm v0.3 (Li 2016) and Flye v2.9.1(Kolmogorov et al. 2019) for assembly generation, and Medaka v1.8.0. (github: nanoporetech/medaka) for polishing. The circular assemblies of chromosomes and plasmids were rotated to *dnaA* and *repA* respectively using dnaapler (Altschul et al. 1990; Bouras et al. 2024) and were submitted to NCBI under the BioProject PRJNA1167355, and annotated by PGAP (Tatusova et al. 2016). Since the initial assembly of Mrh B62 was not circularized, the identical assembly pipeline was followed with lower stringency of downsampling to obtain a circular genome. The *Mycetohabitans* genome assemblies were analyzed for completeness and quality using BUSCO with specifying the lineage as burkholderiales_odb10, and CheckM (v1.2.2) (Parks et al. 2015; Simão et al. 2015).

Phylogenetic and Average Nucleotide Identity Analysis

To compare *Mycetohabitans* genomes to *Burkholderia* sensu lato and related genera of interest, the GTDB-Tk v2.4.0 de_novo_wf command was run with default options and with taxa filters for *Mycetohabitans, Burkholderia, Paraburkholderia, Caballeronia, Trinickia, Pararobbsia, Robbsia, Mycoavidus, Glomeribacter, Pandoraea, and Chitinasiproducens* (Chaumeil et al. 2022). *Pandoraea* was specified as the outgroup. This pipeline pulls from the current GTDB taxonomy and uses the WAG+GAMMA model within FastTree to calculate trees. In total, 383 sequences were aligned using 120 markers based on the 27 *Mycetohabitans* genomes. For average nucleotide identity analysis, representative genomes of each genus in *Burkholderia* sensu lato were retrieved from NCBI (**Table S1**). Together with the *Mycetohabitans* genomes, they were analyzed with FastANI (Jain et al. 2018). For phylogenetic comparisons of chromosomes and plasmids, *dnaA* and *parA* sequences were extracted respectively. Sequences were aligned with MUSCLE within MEGAX (Kumar et al. 2018). Evolutionary history for each group was inferred with the Maximum Likelihood method and Tamura-Nei model, with default parameters and 1000 bootstraps using MEGAX. Final figures for all phylogenetic and ANI analyses were visualized

and polished using FigTree v1.4.4 , RStudio with key package ggtree v3.6.2 (Yu et al. 2017) , and Adobe Illustrator.

Pangenomic analyses

Generation and visualization of the pangenome for 28 *Mycetohabitans* strains was done using Anvi'o v8 (Eren et al. 2020), according to the workflow used by Delmont & Eren (Delmont and Eren 2018). *anvi-script-process-genbank* was used to split GenBank files into FASTAs, external gene calls and functions. For each *Mycetohabitans* genome, contig databases were developed by running *anvi-gen-contigs-database* – which uses Prodigal (Hyatt et al. 2010) – on the FASTA files, with the flag *–exernal-gene-calls* specifying "NCBI_PGAP" as the gene caller. *anvi-import-functions* was used to annotate the contigs databases with the corresponding functions file. Further, *anvi-run-kegg-kofam* was run to further annotate the contig databases with KEGG metabolic pathways. The contig databases were linked using *anvi-script-gen-genomes-file* and made into a unified genomes database using *anvi-gen-genomes-storage*. Pangenome creation and visualization was done using *anvi-pan-genome*, and *anvi-display-pan* respectively, followed by *anvi-compute-genome-similarity* for FastANI (Jain et al. 2018). The pangenome was manually binned into Core, Accessory and Unique gene clusters on the *anvi-interactive* platform based on the number of genomes each gene occurs in. Core gene clusters (GC) were found in a minimum of 28 genomes, accessory in anywhere between 2-28 genomes, and unique in a maximum of one. Identical workflows were used for creating replicon-specific comparisons after splitting the NCBI_PGAP-annotated genbanks into the three contigs using in-house scripts (github: cartercharlotte/Mycetohabitans-pangenome). GenBank files belonging to Mrh B1, Msp B8, Mef B5, and Msp B46 genomes were used to infer synteny using syny (Julian and Pombert 2024).

Heap's law analysis

A gene presence absence matrix was generated from the computed pangenome using the command *anvi-script-gen-function-matrix-across-genomes* with specifying "NCBI_PGAP" as the *–annotation-source* and *–gene-caller*. R scripts were used to compute rarefaction curve for the data stored in matrix using the package vegan (github: vegandevs/vegan).

Transposable Element and Pseudogene analysis

ISEScan was used to infer TE stats on the whole genome FASTA files (Xie and Tang 2017). The .sum output files were then used to plot the percent genome occupied by TEs using R. Pseudogenes predicted during PGAP annotation were collated from the genbank files into a dataframe, and visualized with R (Tatusova et al. 2016). Pearson correlation was performed on the TE and pseudogene percentages to determine whether there is a linear relationship between the two.

dN/dS analysis

FASTA files containing DNA sequences of single-copy core genes (SCG) (Chaumeil et al. 2022) were pulled from the chromosome and chromid genome comparisons using the command *anvi-get-sequences-for-gene-clusters* using the arguments *--report-DNA-sequences* and *--split-output-per-gene-cluster*. These were then aligned using ClustalW (Thompson et al. 1994). R package Ape (Paradis et al. 2004) was used to calculate dN/dS values for each gene in each replicon, using the sequence of each gene in B1 as reference to compare with that gene sequence in the rest of the genomes. Files having non-identical gene sequences were used in these analyses, and the files that didn't have unique sequences were excluded.

antiSMASH and Clinker

Assembled genome FASTA files for all strains were submitted to the antiSMASH v7 bacterial version software (Blin et al. 2023). Strictness level of "relaxed" was selected to identify both well-defined clusters containing all required parts as well as partial clusters missing one or more functional parts. All additional features of antiSMASH were run including KnownClusterBlast, MIBiG cluster comparison, Cluster Pfam analysis, TFBS analysis, ClusterBlast, ActiveSiteFinder, SubClusterBlast, RREFinder, Pfam-based GO term annotation, and TIGRFam analysis. Subsequent results were analyzed based on the cluster type predicted, organization of genes within the cluster, and the most similar known cluster. Genbank files from each cluster predicted by antiSMASH were submitted to clinker (Gilchrist and Chooi 2021) through the command line with the identity threshold between genes being the default 30%. Clinker then performed global alignments between sequences in each cluster, produced a cluster similarity matrix, created optimal ordering by hierarchical clustering, and then output visualizations using clustermap.js. The visualizations were then manually sorted through to identify clusters where the core biosynthetic genes showed similarity as well as the non-core biosynthetic genes in the cluster such as secondary biosynthetic genes, transport, and regulatory genes.

Bacteriophage and CRISPR Prediction

The computational tool geNomad v1.11.1 (Camargo et al. 2024) was run on the set of Mycetohabitans spp. genomes to identify prophage. Predicted phage were quality assessed with CheckV version 1.01.01 (Nayfach et al. 2021) to estimate completeness. Average nucleotide identity analysis was run with FastANI v1.34 (Jain et al. 2018). CRISPRCasFinder was run on each genome to detect Cas proteins and CRISPR arrays using the general clustering model (Couvin et al. 2018).

RESULTS

Long read, complete genome sequences for *Mycetohabitans* strains

We screened *Rhizopus* spp. isolates from the Agricultural Research Service Culture Collection (NRRL) for the presence of endohyphal *Mycetohabitans* strains via PCR. We identified novel strains Mrh B10 and Mrh B203, and confirmed endosymbionts in strains expected to be hosts based on bacterial sequence present in previous short-read fungal

genome sequencing data (Carpenter et al. 2024). Positive cultures were used for extraction of the bacteria, and then genomic DNA preparation for Oxford Nanopore Technologies long-read sequencing. In total, we sequenced and assembled genomes for 20 bacterial strains (**Table 1, Table S2, Figure S1**), including Msp B46 which we re-sequenced due to our previous PacBio assembly not resolving into complete replicons (Carpenter et al. 2024) and the type strain Mrh B1 which was previously available as short-read Illumina assembly (Lackner et al. 2011). For re-sequenced strains, our new ONT assemblies had average nucleotide identity (ANI) values of greater than 99.97% to their respective previous assemblies, indicating robust base calling (Jain et al. 2018).

The genome sizes range from 3.3 Mbp to 3.8 Mbp, and all genomes were considered complete with BUSCO scores upward of 98.8% and having resolved into circular replicons. The genomes all had lower than 0.6% contamination as reported via CheckM (Parks et al. 2015). The GC content of all *Mycetohabitans* strains lies at ~60%. (**Table 1**). All *Mycetohabitans* genomes have two stable replicons – a chromosome (~2.7 Mbp) and a chromid (~700-900 kbp). A plasmid of size range ~100-200 kbp is only found in 12 strains. For analyses in this study, we considered a pangenomic dataset of 28 total long read *Mycetohabitans* genomes (**Table S2**) comprised of these new ONT assemblies and our previous PacBio assemblies (Carpenter et al. 2024).

Table 1. *Mycetohabitans* spp. genomes sequenced and assembled in this study.

Bacterial strain	Genome size	Coverage	BUSCO score	%GC	# of replicons	Host accession	Nucleotide accession
M. rhizoxinica B2	3853378	108x	99.4%	59.59%	3	ATCC 20577	CP176780-CP176782
Mycetohabitans sp. B8	3404497	100x	99.4%	60.08%	2	CBS 308.87	CP173344-CP173345
M. rhizoxinica B10	3429290	108x	99.4%	60.07%	2	NRRL 2710	CP176778-CP176779
M. rhizoxinica B203	3429291	108x	99.4%	60.07%	2	NRRL 6203	CP176776-CP176777
M. endofungorum B23	3642467	111x	99.2%	59.76%	3	NRRL 62023	CP184774-CP184776
M. endofungorum B29	3355370	107x	99.1%	60.22%	2	NRRL 13129	CP173342-CP173343
M. rhizoxinica B34	3650605	101x	99.3%	59.97%	2	NRRL 2934	CP173340-CP173341
Mycetohabitans sp. B46	3327273	102x	99.4%	60.03%	2	NRRL 5546	CP173320-CP173321
M. rhizoxinica B48	3371874	100x	99.2%	59.92%	2	NRRL 5548	CP173338-CP173339
M. rhizoxinica B50	3532824	100x	99.3%	59.93%	2	NRRL 5550	CP173336-CP173337
M. endofungorum B51	3754811	105x	99.6%	59.47%	3	NRRL 5551	CP173333-CP173335
M. rhizoxinica B514	3853403	111x	99.4%	59.59%	3	NRRL 1514	CP176773-CP176775
M. rhizoxinica B52	3623805	105x	99.1%	59.89%	2	NRRL 5552	CP173331-CP173332
M. endofungorum B53	3608068	87x	99.3%	59.78%	3	NRRL 5553	CP173328-CP173330
M. rhizoxinica B55	3528370	99x	99.4%	59.87%	3	NRRL 6255	CP173325-CP173327
M. rhizoxinica B58	3668316	97x	98.8%	59.72%	3	NRRL 5558	CP184771-CP184773
M. rhizoxinica B62	3429197	116x	99.4%	60.07%	2	CBS 339.62	CP178341-CP178342
M. endofungorum B75	3642023	102x	98.9%	59.71%	3	NRRL 66675	CP173322-CP173324
M. rhizoxinica B82	3454439	102x	99.1%	59.92%	2	NRRL 2582	CP184791-CP184792
M. rhizoxinica B1	3749950	105x	99.3%	59.71%	3	ATCC 62417	CP184277-CP184279

Mycetohabitans **strains have atypical natural boundaries for average nucleotide identity**

In recent genomic studies of *Burkholderia* sensu lato, *Mycetohabitans* strains were underrepresented due to the lack of available genomes (Bach et al. 2022; Bach et al. 2023; Mullins and Mahenthiralingam 2021). We used the Genome Taxonomy Database to phylogenetically analyze a representative set of *Burkholderia* sensu lato genomes. We also included those from closely-related *Mycoavidus* and *Glomeribacter* genera given their niche as endofungal bacteria and used *Pandoraea* as an outgroup (**Figure 1A**). The genus *Candidatus* Vallotia made up of bacterial symbionts of adelgids was previously proposed to be consolidated with *Mycetohabitans* (Dial et al. 2022; Szabó et al. 2022)*; Candidatus* Vallotia strains are now listed in the Genome Taxonomy Database as *Mycetohabitans* and were thus included in our phylogenetic analysis. Based on the data in **Figure 1**, we have chosen to label them as *Candidatus* Vallotia and differentiate them from *Mycetohabitans,* further commented on in the discussion.

The *Mycetohabitans* genus forms a strong clade that is further validated by ANI analysis (**Figure 1B**). Inter-genus comparisons within *Burkholderia* sensu lato fall around 77-80%. There is a discontinuity that begins around 83%, the expected beginning of the range for inter-species comparisons, but the intra-genus *Mycetohabitans* comparisons then span from 90% to >99% (**Figure 1C**). Comparisons between the type strain of Mef (B5) and Mrh strains are 90.7-91.9%, a rare range for ANI values (Jain et al. 2018; Konstantinidis 2023). The orphan strains Msp B46 and Msp B8 share ~92.5% ANI and ~91.5% with Mrh and ~90% and ~90.5% with Mef*,* respectively. Mrh strains share >97% ANI, with the exception of B23 and B48 that are only 95.2% ANI with the other Mrh strains. Similarly, Mef has two strong clades in **Figure 1A**, with the type strain B5 sharing only 94.2-96.2% ANI with all but one strain (B29; >99% ANI). However, other strains in the two subclades share 95.5-96% ANI, such as B13 and B75 sharing 96% ANI, supporting that this is one species, with a potential subspecies structure.

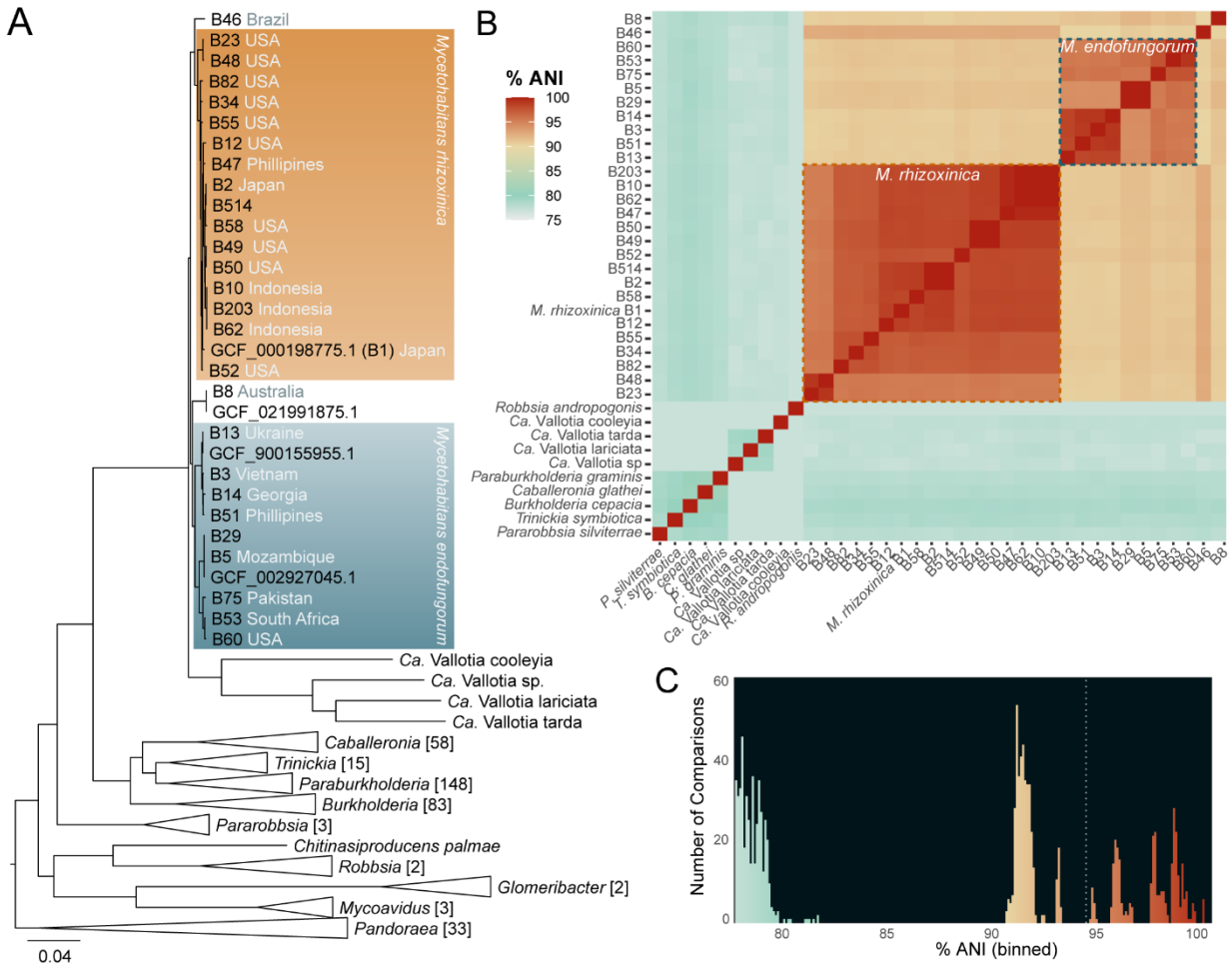

Figure 1. Taxonomic placement of *Mycetohabitans* strains within *Burkholderia* sensu lato. **A**. An approximately-maximum-likelihood tree for *Mycetohabitans* genomes and representatives from closely related genera provided by the Genome Taxonomy Database. Branches that contained a single genus were collapsed and the number of taxa within is displayed in brackets, except for the *Mycetohabitans* and *Ca.* Vallotia clades. Branch length indicates substitutions per site. When known, the country of origin is indicated for the host fungus of each *Mycetohabitans* strain (**Table S2**). **B**. Average nucleotide identity (ANI) comparisons of the *Mycetohabitans* genomes to each other and representative strains from *Burkholderia* sensu lato (accession numbers in **Table S1**). Dotted lines enclose comparisons between the same species of *Mycetohabitans*. **C**. Count data for the ANI values in panel B binned by 0.1. A dotted line indicates the natural gap at 94%.

***Mycetohabitans* genomes show high synteny within replicons across strains**

To investigate syntenic conservation across *Mycetohabitans*, we compared Mrh type strain B1 and Mef type strain B5 with the two isolates that did not fall into either named species, Msp B8 and Msp B46. We found highly syntenic chromosomes, with somewhat less synteny

observed in the chromids (**Figure 2A**). There were examples of syntenic DNA sections between chromosome and chromid, mostly notably the chromid in Msp B8 has some elements syntenic with the Mrh B1 chromosome. In this analysis, Mrh B1 is the only strain that has a 3rd replicon, the plasmid, which does have smaller syntenic blocks from the chromosomes or chromids of the other strains.

The *Mycetohabitans* genus forms an open pangenome

To holistically explore the diversity of our 28 *Mycetohabitans* genomes, we generated an Anvi'o pangenome (**Figure 2B, Table S3**). 79,578 gene calls were clustered into 4652 gene clusters (GC) which were further categorized as single-copy core GCs (SCG), core GCs, accessory GCs and unique GCs. While the SCGs were characterized by the program, core, accessory and singleton GCs were manually curated based on presence of the GC in all 28 genomes, 2 to 27 genomes, or only 1 genome, respectively. There were 1752 core GCs with 52,055 gene calls (37.6%), 2207 accessory GCs with 26814 gene calls (47.44%) and 693 singleton GCs with 707 gene calls (14.89%). The categories cell wall mobility, translation, transcription, mobilome, signal transduction and defense mechanisms have high % gene presence in the *Mycetohabitans* genome (**Figure S4**). A Heap's Law model (Tettelin et al. 2008) was used to estimate whether the *Mycetohabitans* pangenome is open or closed. Since the number of new genes increases upon addition of more genomes (as indicated by the α of 0.1), the *Mycetohabitans* genus forms an open pangenome (**Figure 2B**).

Transposable element and pseudogene content are correlated *Mycetohabitans* strains

Using the PGAP annotations for each of the genome, we computed the percentage of coding gene sequences (CDS) that are frameshifted, incomplete, or contain internal stop codons (Tatusova et al. 2016). The total putative pseudogene content ranged from 6.4% in Mrh B47 genome to 9.96% in Mef B13. Mef B14, B75, and B51 – strains with the longest plasmids of lengths 201412, 181953, and 231357 respectively – have 9.95%, 9.86% and 9.56% of their CDS putatively pseudogenized (**Figure 2C, Figure S3, Table S4**). However, this pattern of correlation between plasmid length or presence, and pseudogene content is not consistent across all genomes. Mef B75 also had the highest percentage (6.36%) of its genome masked by transposable elements (TEs), and Mrh B48 had the least, 1.58% (**Figure 2D, Table S4, Figure S2**). We wanted to check whether there is a correlation between TE and pseudogene content across the *Mycetohabitans* strains. Mef B75 and B51 both fall at the higher end of TE and pseudogene content, Msp B46, Mrh B47, B48, B49 and B50 all have both – low TE and pseudogene content (**Table S3, Figure 2C**). Interestingly Mef B60 has the second highest TE content of 4.53%, and falls towards the lower end of pseudogene content (**Table S4, Figure S2-3**).

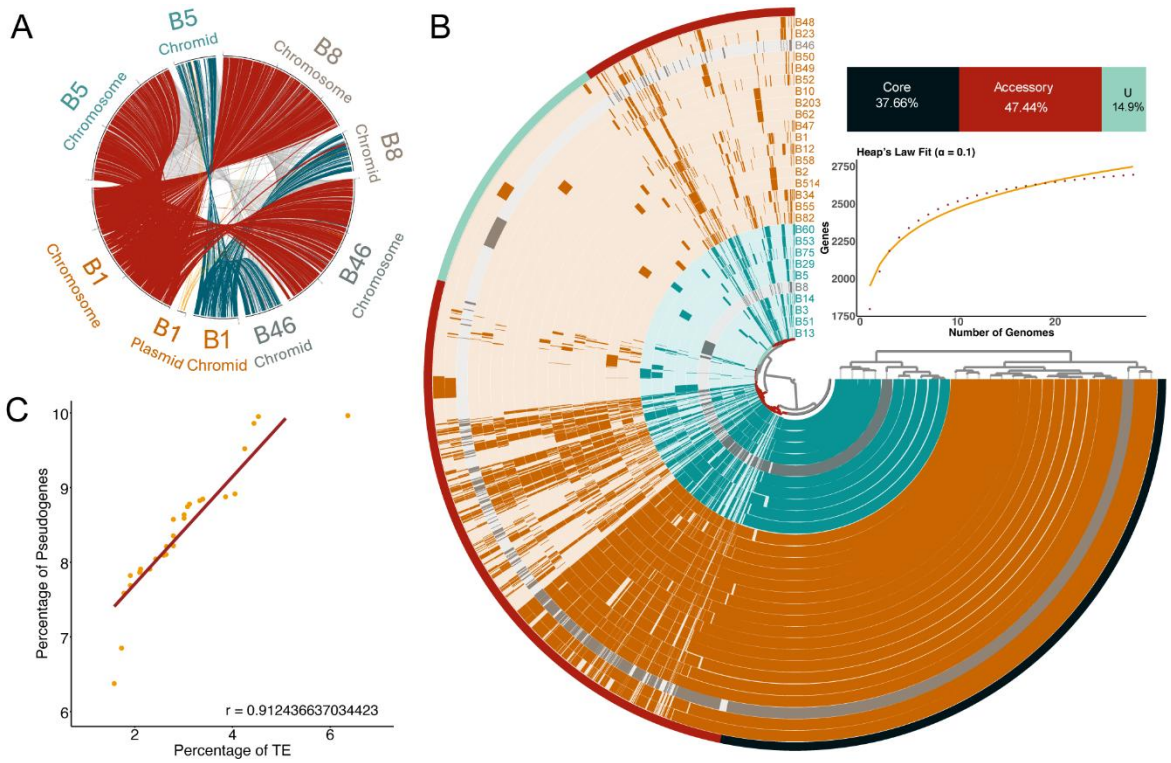

Figure 2. Genome synteny and content comparisons across the *Mycetohabitans* genus **A**. Synteny comparison between replicons from the *Mycetohabitans rhizoxinica* (Mrh) B1, *Mycetohabitans endofungorum* (Mef) B5, *Mycetohabitans* sp. (Msp) B8, and Msp B46 genomes with B1 treated as the reference. Deep red connectors represent chromosome, deep blue chromids, and orange plasmid. **B**. Anvi'o plot illustrating the *Mycetohabitans* pangenome, with each ring representing one complete genome. The inner dendrogram shows hierarchical clustering of gene clusters (GC). Core GCs (black), accessory GCs (deep red) and unique GCs (cyan) are marked as the outermost circle and their percentage in the pangenome is summarized in the stacked bar chart, below which is a Heap's law fit. **C.** Correlation plot between percent of genome masked by transposable elements (TEs) and percent of coding DNA sequences (CDS) that are pseudogenized. Pearson coefficient (r) is indicated at the bottom right of the plot. In all panels where relevant, *M. rhizoxinica* strains are indicated in orange, *M. endofungorum* in teal, and *M.* sp. in grey.

Chromids show lower conservation than chromosomes

Though originally described as a megaplasmid in the Mrh B1 genome, the presence of the secondary replicon and its conservation across *Mycetohabitans* strains supported a more stable role as a chromid (Harrison et al. 2010; Lackner et al. 2011). To assess the structural makeup of the pangenome, we created single replicon comparisons using the same Anvi'o pipeline used in the whole-genome pangenome creation for **Figure 1B** (Eren et al. 2020). Anvi'o identified 3500 and 1335 GCs in the chromosomes and chromids, respectively (**Figure 3A-B**). The hierarchichal clustering based on GC frequencies within the two replicons group the strains similarly, with the exception that Msp B8 changes positions

significantly by clustering with Mrh chromosomes, but Mef chromids. The chromosome has a higher fraction of core GCs compared to the chromids which are conversely more enriched in accessory gene content (**Figure 3A-B**).

As the differential amount of GC conservation suggests differential rates of evolution, we estimated the accumulation of non-synonymous (dN) to synonymous (dS) mutations in these replicons (Kryazhimskiy and Plotkin 2008). We calculated the dN/dS values for single-copy core genes in all *Mycetohabitans* strains that had non-identical sequences to B1, and plotted all those data points for each of the two replicons (**Figure 3C**). While greater dN/dS ratio indicates diversifying selection or adaptive evolution, a lower value would support higher selective or purifying forces acting on the replicon. The dN/dS ratio of chromid genes distributes similarly to that of the chromosome , supporting the description as a chromid and not a megaplasmid (Harrison et al. 2010). We further validated this distinction by comparing the guanine-cytosine content (%GC) between chromids and chromosomes of the same strain. The %GC of the chromid is on average 1.65% lower than that of the chromosome (**Figure 3D; Table S5**).

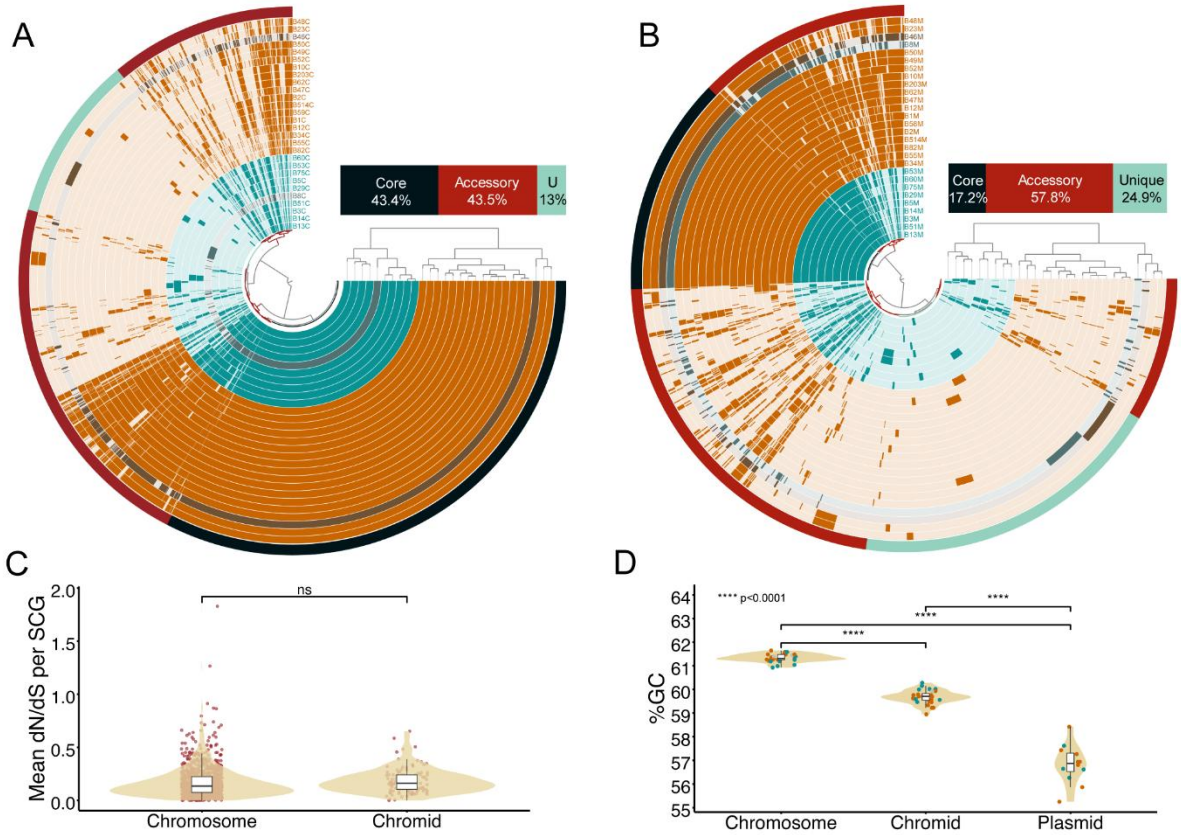

Figure 3. Comparisons between replicons i.e. chromosome, chromid and plasmid across *Mycetohabitans*. Anvi'o plots to compare **A.** chromosomes and **B**. chromids across the strains. Each ring represents one *Mycetohabitans* strain's relevant replicon and the inner dendrogram shows hierarchical clustering of gene clusters (GC). Core GCs (black),

(cont.) accessory GCs (deep red) and unique GCs (cyan) are marked as the outermost circle and their percentage in the pangenome is summarized in the stacked bar chart. **C**. dN/dS value distribution for non-identical single-copy core genes in chromosomes and chromids **D.** Guanine-cytosine (%GC) content of each replicon is shown as a percentage with individual data points colored by species. P-value notations determined by T-test are indicated on the plot as asterisks. In all panels where relevant, *M. rhizoxinica* strains are indicated in orange, *M. endofungorum* in teal, and *M.* sp. in grey.

Mycetohabitans **plasmids are dynamic accessory gene hubs that are potentially lost or transferred**

A similar comparative analysis of the 12 *Mycetohabitans* plasmids using Anvi'o identified 362 GCs: 8 core, 218 accessory, and 136 unique GCs (**Figure 4A**). The largest plasmid, Mef B51, has the highest number of genes and unique GCs. Out of the eight core GCs, only four are classified as single-copy core genes (SCGs) (Parks et al. 2018), emphasizing the highly accessory nature of plasmid GCs. We binned plasmid gene clusters into mobilome-related components and found 45 GCs related to transposases, 20 GCs related to conjugation machinery/Type IV Secretion System, and 2 GCs related to bacteriophage genome fragments (**Figure 4A**). Furthermore, 55 GCs related to toxin-antitoxin systems were identified, with 2 of these GCs forming the core of the plasmid pangenome belonging to the type II toxin-antitoxin system. Specifically, these are RelE/ParE family toxin and RelB antitoxin. One of the accessory GCs contains *btl* genes which are known type III secretion system effector proteins that vary in number, sequence, and genomic location between strains (Carpenter et al. 2024; Carter et al. 2020). As no other effector proteins are validated, we did not further explore the diversity or genomic location of type III effectors.

To check the conservation of plasmids within bacterial lineages and assess the possibility of horizontal exchange, we created phylogenetic trees based on core replication genes: the *parA* gene found on plasmid and the *repA* gene on the chromosome (**Figure 4B**)**.** Within Mef, plasmid presence and relatedness mirrors the chromosome topology and is monophyletic. Yet, plasmid loss likely occurred in strains such as Mef B13 and B3 which cluster with plasmid-containing strains despite lacking plasmids themselves. However, within Mrh, there is more discord, as which strains do or do not have a plasmid is not as clearly clustered. Mrh B1 stands out with the most divergent plasmid from other Mrh strains, contrasting with the strain's overall close relatedness with Mrh B12 (**Figures 1-2**). That Mrh B12 and B1 have such distinct plasmids suggests plasmid horizontal transfer has occurred within the Mrh lineage, a hypothesis that is further supported by B23 and B58 having similar plasmids despite their overall divergence.

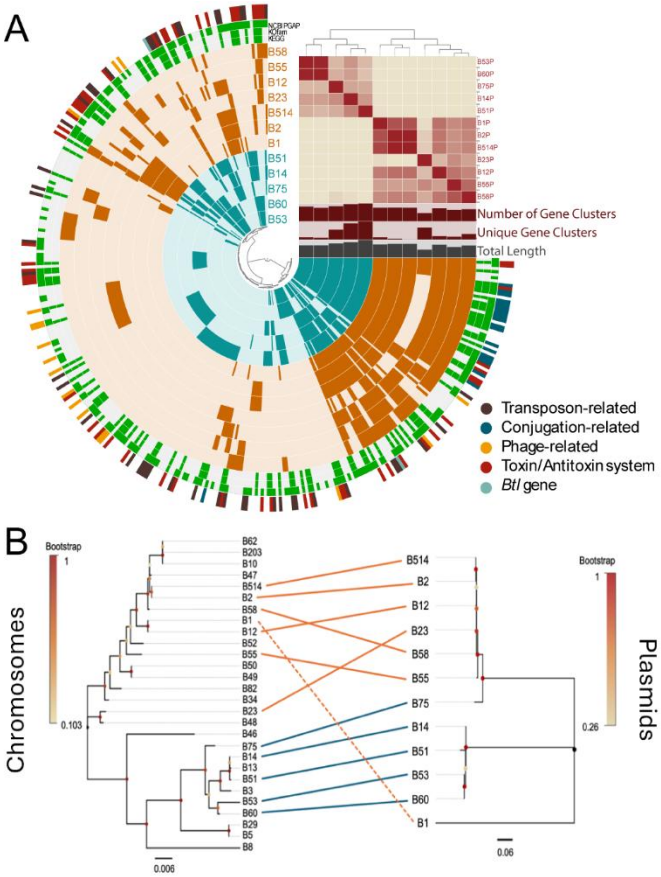

Figure 4. Analysis of the inconsistently present third replicon across *Mycetohabitans* strains. **A.** Anvi'o plot of *Mycetohabitans* plasmids indicated as individual rings, with toxin/antitoxin system, *btl* type III effector gene, and mobilome-related GCs annotated on the outermost circle colored according the panel key. Average nucleotide identity (ANI) of the plasmids is depicted as a heat map. Bar plots show the total lengths and number of GCs (unique and overall) for each plasmid sequence. The inner dendrogram shows hierarchical clustering of GCs. **B.** Co-phylogeny comparing topology of *dnaA* relationship across chromosomes (left) to *parA* relationship across plasmids (right) inferred by Maximum Likelihood with MEGAX. Dots at inner nodes of trees represent bootstrap values as a fraction of 1000 bootstaps. In all panels where relevant, *M. rhizoxinica* strains are indicated in orange, *M. endofungorum* in teal, and *M.* sp. in black.

***Mycetohabitans* spp. are enriched in diverse biosynthetic gene clusters, with many associated with nonribosomal peptides**

From previous studies, it is known that *Mycetohabitans* spp. have a high percentage of their genome devoted to biosynthetic gene clusters (BGCs) compared to other species in *Burkholderia* sensu lato (Mullins and Mahenthiralingam 2021) . We identified a total of 373 unique biosynthetic gene clusters (BGCs) across the 28 *Mycetohabitans* strains using antiSMASH (Blin et al. 2023). All strains were predicted to have BGC clusters for a terpene, a terpene/phosphonate, ribosomally synthesized lassopeptides, and numerous distinct nonribosomally synthesized peptides (NRPs) (**Figure 5A**). The majority of BGCs were found in chromosomes and chromids, with only two clusters predicted in plasmids: NRP group 29 in Mef B51 and NRP group 27 in Mef B75 (**Figure 5B; Table S6**). The classic rhizoxin cluster that led to the discovery of this genus was putatively found in all strains except Mrh B82 (Partida-Martinez and Hertweck 2005; 2007). B8 was the only strain predicted to have a hybrid polyketide synthase (PKS) and NRPS cluster other than rhizoxin, which produces necroximes (Niehs et al. 2020). The conservation of predicted ribosomally synthesized lassopeptide BGCs align with previous findings on a smaller set of genomes showing loci with homology to those from type strain B1 that produce burhizin-23, mycetohabin-16, and mycetohabin-15, though their ecological role remains unknown (Bratovanov et al. 2020).

We used Clinker (Gilchrist and Chooi 2021) to further group the secondary metabolite clusters beyond the initial predictions by antiSMASH, based on similarity in core biosynthetic genes and surrounding regulatory, additional biosynthetic, and transport genes. Not all NRP clusters grouped by Clinker are equally similar and clusters within a group possibly encode for different secondary metabolites. In total, there were 26 similar groups, with NRP Groups 8, 18, 28, 30, and 31 being unique/singleton BGCs. However, some BGCs are represented twice within **Figure 5B** if they were predicted to have genes for both an NRPS and another secondary metabolite product, such as phenazine. Although NRP Group 1 clusters are found across all strains, this cluster has some variety in structure with some BGCs having additional biosynthetic genes, suggesting further study is needed to assess expression and metabolite variation (**Figure S5**). NRP Group 11 clusters, found mostly in Mrh strains, have an NRPS with similarity greater than 90% to the *habA* gene (Niehs et al. 2022). NRP Group 10 clusters are found across most strains and have core NRPS genes that are between 96-100% similar to the NRPS in the previously characterized rhizomide cluster (Wang et al. 2018). NRP Group 9 is highly conserved and was found in all Mrh strains as well as B23 and B46. Since it does not have similarity to the NRPSs of endopyrrole A cluster nor rhizomide (**Figure S6**), this may be encoding a novel NRP of interest.

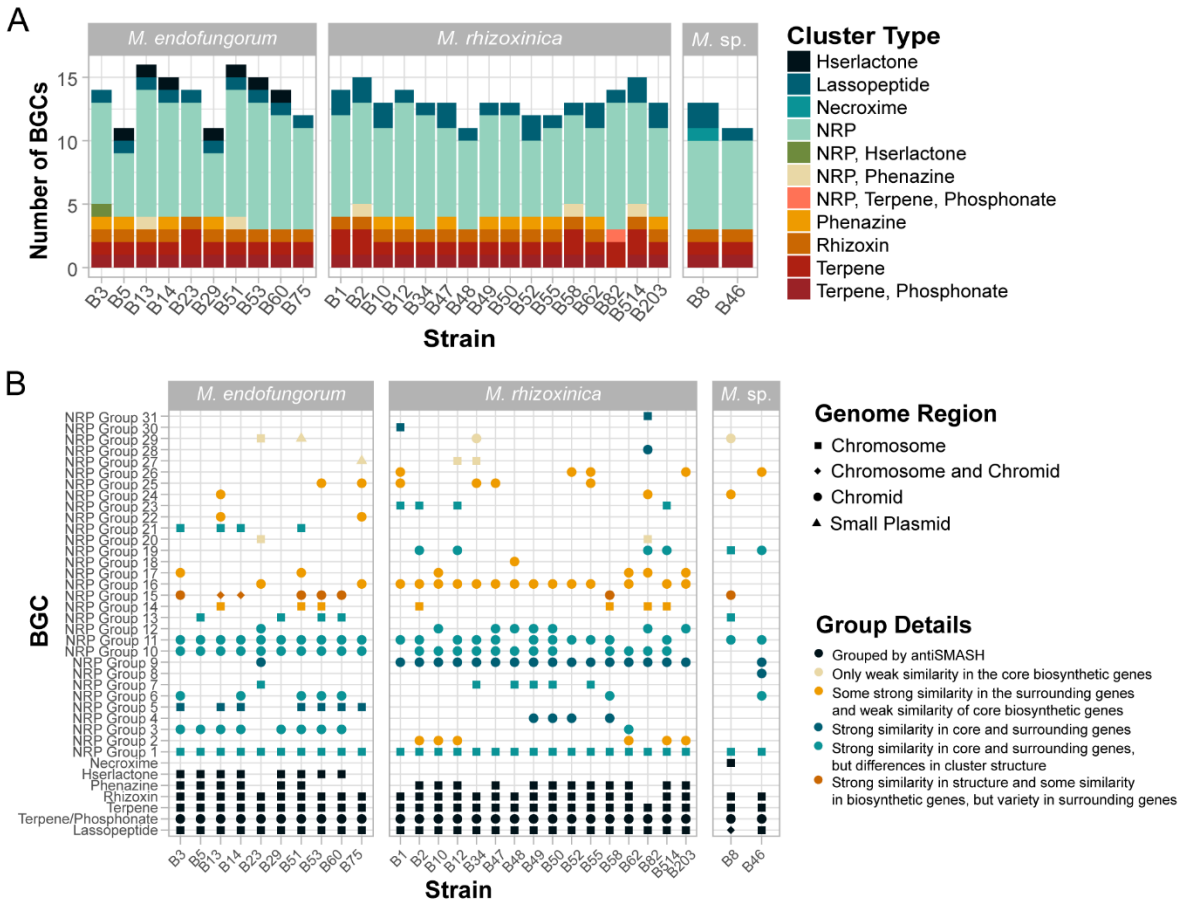

Figure 5. Prediction of biosynthetic gene clusters (BGCs) in *Mycetohabitans* genomes. **A**. Fractions of the types of BGC found in *Mycetohabitans* strains, grouped by species and colored by cluster type. **B**. Similarity of BGCs across *Mycetohabitans* strains and the replicons they are found in. Dots are annotated by shape and color to communicate genome region found in as well as similarity metrics. All underlying data and additional information like genomic location is in **Table S6**. NRP; nonribosomal peptide.

Most *Mycetohabitans* spp. genomes have putative intact prophage

We surveyed each genome for CRISPR-Cas systems that may serve as antiphage defenses and found no *cas* operons in any strain. A subset of the strains had low-confidence, single spacer CRISPR arrays, but these had no repeat similarity between them and likely represent false positives. We thus hypothesized that the genomes may contain intact prophage. Across the set of *Mycetohabitans* spp. genomes, all were predicted to have viral sequences on their chromosomes (**Figure 5A**), but not on the chromid or plasmids. 60 prophage sequences were found, 36 of which were designated as high quality (predicted to be >90% complete). Seven genomes did not have any high-quality prophages: Msp B8, Mrh B82, Mrh B55, Mrh B48, Mef B5, Mef B60, and Mef B29. We ran ANI analysis to briefly assess the relationship of the high-quality prophages (**Figure 5B**). The predicted phages tend to cluster in two distinct groups, except phage B34-2 which fell outside of both groups. Overall, Mrh tends to have a greater quantity of predicted higher quality phages, and Mef has a few strains

with just viral genome fragments. Due to the novel nature of these phages, functional annotations within the prophage genes are mostly limited to standard structural components such as head proteins, tail, baseplate, etc. However, some of the genomes in the smaller of the two ANI clusters (upper right) have putative toxin/antitoxin genes and some on the middle group within the larger cluster has NtrX-like response regulators, suggesting possible functional outcomes from phage presence.

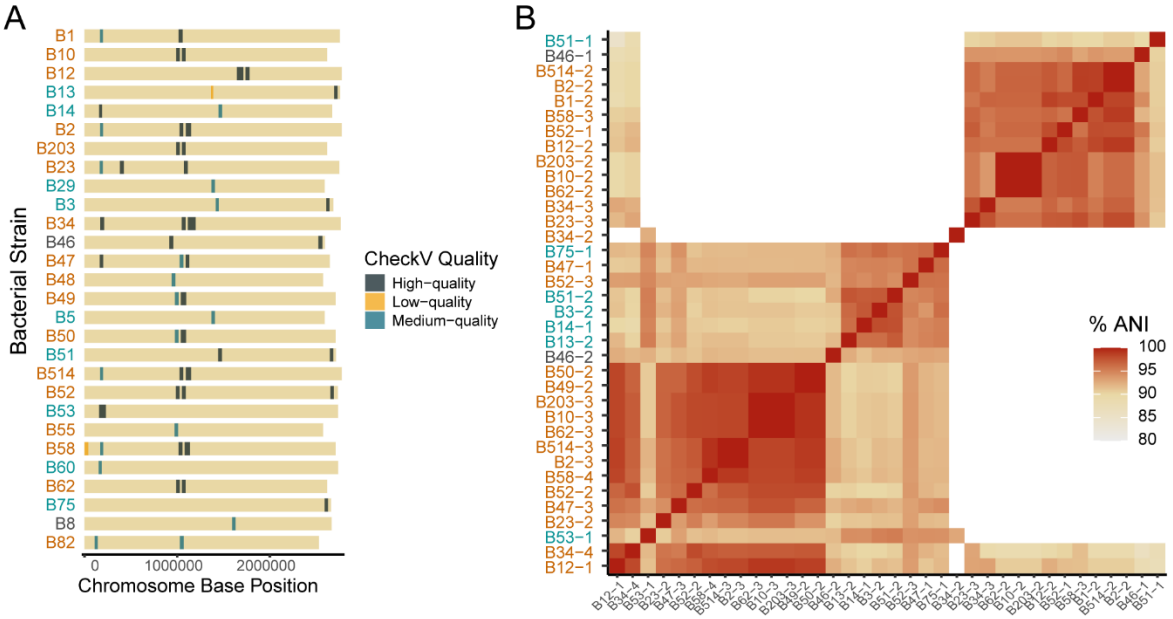

Figure 6. Predicted prophage regions in the *Mycetohabitans* spp. genomes. **A.** Simplified chromosome map for each strain showing the location of putative prophages indicated based on their quality score by CheckV. **B.** Average nucleotide identity (ANI) of all high-quality prophages identified across the 28 genomes, each indicated by the strain name and an identifying number. In all panels, *M. rhizoxinica* strains are indicated in orange, *M. endofungorum* in teal, and *M.* sp. in black.

DISCUSSION

With this study, we aimed to uncover the genome dynamics during the transition of an endosymbiotic bacterium from facultative to obligate, using the endofungal *Mycetohabitans* genus as a model. By sequencing genomes with high quality, long-read Oxford Nanopore Technology sequencing we were able to dramatically increase the genomic resources available for this genus and conduct a more structurally focused assessment. Although *Mycetohabitans* are known to have low unique gene content compared to *Burkholderia* sensu lato, we still see an open pangenome with accumulation of non-essential and/or pseudogenes, a phenomenon typically observed in genomes of recently host-restricted endosymbionts (Bach et al. 2022; Dewar et al. 2024; Grujcic et al. 2025; Hendry et al. 2018; Lind et al. 2018; McCutcheon and Moran 2012). Added to this, the common trait of BGC enrichment resembles genome expansion of genes relevant to the role within a host, as demonstrated by insect symbiotic *Arsenophonus* spp. (Siozios et al. 2024).

In many symbionts, seemingly non-core genes contributing to host functionality are conserved despite genome loss (Carlier et al. 2016). Overall, our pangenomic data for *Mycetohabitans* supports a hypothesis of expansion of transposable elements and BGCs, in the midst of genome reduction occurring via pseudogenization and likely the loss of the third replicon, though without as dramatic an expansion of pseudogenes and TEs as have been observed in other endosymbionts.

Our investigation of ANI across the *Mycetohabitans* genomes revealed high intragenus identity with less clear species boundaries. As two species have been named for the *Mycetohabitans* genus, we propose conserving these species designations and setting the ANI thresholds for *Mycetohabitans* spp. at 94% to indicate species based on the observed areas of discreteness (Konstantinidis 2023). Though bacterial species are a complex concept, the assignment of this species boundary also aligns with the finding that homologous recombination efficiency decreases dramatically by 90% nucleotide identity (Power et al., 2021; Konstantinidis, 2023); though, genetic exchange within this genus has not been explicitly investigated. Species boundaries within endosymbiotic genera are not well delineated, generally, and require more pangenomic studies and functional studies to assess diversity and grapple with how to define species. For example, the highly studied *Wolbachia* genus is divided into various monophyletic "supergroups" with genomes that have ~93% or higher identity within them and appear to have undergone host switching across insect species (Mahmood et al. 2023; Vancaester and Blaxter 2023; Wang et al. 2020). Many other endobacteria from single host species have high ANI values of >99% across genomes, such as those from the scaly-foot snail (*Chrysomallon squamiferum*) and the deep-sea mussel (*Gigantidas platifrons*) (Lan et al. 2022; Sun et al. 2023).

Within the historical context of continued efforts to appropriately taxonomically classify members of the diverse *Burkholderia* genus, we find that our data supports *Vallotia* remaining its own genus, in contrast to the proposal to combine it with *Mycetohabitans* (Szabó et al. 2021). Our analysis of *Burkholderia* sensu lato with all available *Mycetohabitans* and formerly *Candidatus* Vallotia genomes clearly shows that the two genera form distinct clades and have ANI separation (**Figure 1**). This conclusion is further supported by the significant genome reduction in *Vallotia* compared to *Mycetohabitans* and complete difference in niche, as all sequences assigned to *Vallotia* are from adelgids (Insecta: Hemiptera: Adelgidae), while all *Mycetohabitans* strains are fungal-associated. That these two genera are both endosymbionts that have undergone clear specialization for their unique hosts serves as an interesting natural, evolution experiment and thus could be further compared for insights into signatures of endosymbiosis. Further comparative analyses incorporating *Mycoavidus* and *Glomeribacter*, or other Burkholderia-related endosymbionts would yield more insights as well (Amses et al. 2023; Uehling et al. 2017).

Like many other *Burkholderia* species, *Mycetohabitans* has a multi-partite genome (Bach et al. 2022; diCenzo and Finan 2017). Small syntenic blocks between the Mrh B1 plasmid with chromosomes and chromids of other genomes (**Figure 2A**) suggests potential recombination events between the chromosome, chromid, and plasmid, especially as the

plasmid has been lost from some strains. The plasmids, being enriched in transposases (**Figure 4A**) may be functioning as a recombination hotspot, mediating gene loss (Hendry et al. 2018). We are considering the secondary replicon that is conserved across genomes to be a chromid (Harrison et al. 2010). Though some guidance suggests that %GC variation between chromosomes and chromids should be less than 1% (diCenzo and Finan 2017), we compare the much higher differences between the plasmid and the chromosome (on average 4.43%) to our average 1.65% difference between the chromid and chromosome. Ultimately, the *Mycetohabitans* chromid has chromosome-like evolutionary dynamics including low diversifying evolution rate, and a similar GC content (**Figure 3C-D, Table S6**), as well as conservation of genes involved in core metabolism like transcription and signal transduction (**Figure S4**). Conversely, it shows plasmid-like gene content including toxin-antitoxin maintenance system, partitioning system, mobilome, and relatively high accessory gene content compared to the chromosome (**Figure 3A-B**).

Despite having numerous transposable elements and putative prophage, *Mycetohabitans* spp. genomes did not have any CRISPR-Cas systems, which are implicated in controlling deleterious mobile genetic elements (Westra and Levin 2020). Yet, this aligns broadly with *Burkholderia* sensu lato, as most members have orphan CRISPR arrays with no *cas* operons, or no arrays at all (Pratama et al. 2018; Seo et al. 2015). The extensive presence of toxin-antitoxin systems on the plasmids enabling their maintenance, combined with the lack of CRISPR-Cas systems may be allowing the bacteria to carry out sustained mobilization-mediated gene loss via pseudogenization (Siozios et al. 2024; Vigil-Stenman et al. 2015). However, how many transposons are actually functional is also to be questioned (Cordaux 2009), and conclusions about pseudogenization would require further studies with data assessing transcriptional activity (Goodhead et al. 2020). The presence of mobile genetic elements also supports horizontal gene transfer, such as type III effector acquisition and/or functionalization towards symbiosis maintenance (Carpenter et al. 2024; Carter et al. 2020; Dale et al. 2001; Siozios et al. 2024).

This repertoire of *Mycetohabitans* genomes is derived from Rm isolates sampled from across the world, and the isolates within are accessible through public culture collections. The majority of the samples are from United States and Southeastern Asia, which represents a strength in covering diversity from these areas but a potential gap in other regions. The orphan strains Msp B8 and B46 are the only samples from Australia and South America, respectively, which may underlie their lack of identity with the named species and supports continued sampling and sequencing to capture missing diversity. Especially given that Msp B8 is the only strain predicted to produce necroximes through a BGC, though other endosymbionts in other genera do, supporting the hypothesis of undiscovered diversity on continents in the global south (Büttner et al. 2021; Niehs et al. 2020). Additionally, we do not well understand the diversity represented within *Rhizopus* host fungi of *Mycetohabitans,* or the rate of horizontal transmission of symbionts. Connecting the bacterial genomic data presented here with improved fungal genomic resources and phylogenetics is a natural next step towards understanding how *Mycetohabitans* genetic diversity and speciation has been impacted by host organisms.

Data availability

All genomes assembled in this work are available at NCBI and raw sequencing reads at SRA under the BioProject ID PRJNA1167355; individual nucleotide accessions are indicated in Table 1. All scripts and code used are available at github.com/cartercharlotte/Mycetohabitans-pangenome. Accession information for genomic data not generated in this study, but used for analyses, is listed in Tables S1 and S2.

Funding

This research was sponsored by start-up funding from UNC Charlotte to MEC.

Acknowledgements

The authors thank the UNC Charlotte EVOLVE group, Md Moinuddin Sheam (UNC Charlotte), and David Baltrus (University of Arizona) for critical discussion of data analysis, the USDA ARS NRRL for providing fungal isolates, and the UNC Charlotte University Research Computing group for computational resources.

References

Altschul SF, Gish W, Miller W, Myers EW, Lipman DJ. 1990. Basic local alignment search tool. J Mol Biol. 215(3):403-410.

Amses K, Desiró A, Bryson A, Grigoriev I, Mondo S, Lipzen A, LaButti K, Riley R, Singan V, Salazar-Hamm P et al. 2023. Convergent reductive evolution and host adaptation in mycoavidus bacterial endosymbionts of mortierellaceae fungi. Fungal Genetics and Biology. 169:103838.

Bach E, Sant'Anna FH, Seger G, Passaglia LMP. 2022. Pangenome inventory of *Burkholderia* sensu lato, *Burkholderia* sensu stricto, and the *Burkholderia cepacia* complex reveals the uniqueness of *Burkholderia catarinensis*. Genomics. 114(1):398-408.

Bach E, Volpiano CG, Sant'Anna FH, Passaglia LMP. 2023. Genome-based taxonomy of *Burkholderia* sensu lato: Distinguishing closely related species. Genet Mol Biol. 46(3 Suppl 1):e20230122.

Blin K, Shaw S, Augustijn HE, Reitz ZL, Biermann F, Alanjary M, Fetter A, Terlouw BR, Metcalf WW, Helfrich EJN et al. 2023. Antismash 7.0: New and improved predictions for detection, regulation, chemical structures and visualisation. Nucleic Acids Research. 51(W1):W46-W50.

Bouras G, Grigson SR, Papudeshi B, Mallawaarachchi V, Roach MJ. 2024. Dnaapler: A tool to reorient circular microbial genomes. Journal of Open Source Software. 9(93):5968.

Boyd BM, James I, Johnson KP, Weiss RB, Bush SE, Clayton DH, Dale C. 2024. Stochasticity, determinism, and contingency shape genome evolution of endosymbiotic bacteria. Nature Communications. 15(1):4571.

Bratovanov EV, Ishida K, Heinze B, Pidot SJ, Stinear TP, Hegemann JD, Marahiel MA, Hertweck C. 2020. Genome mining and heterologous expression reveal two distinct families of lasso peptides highly conserved in endofungal bacteria. ACS Chem Biol. 15(5):1169-1176.

Büttner H, Niehs SP, Vandelannoote K, Cseresnyés Z, Dose B, Richter I, Gerst R, Figge MT, Stinear TP, Pidot SJ et al. 2021. Bacterial endosymbionts protect beneficial soil fungus from nematode attack. Proceedings of the National Academy of Sciences. 118(37):e2110669118.

Cabrera-Rangel JF, Mendoza-Servín JV, Córdova-López G, Alcalde-Vázquez R, García-Estrada RS, Winkler R, Partida-Martínez LP. 2022. Symbiotic and toxinogenic *Rhizopus* spp. isolated from soils of different papaya producing regions in mexico. Frontiers in Fungal Biology. 3.

Camargo AP, Roux S, Schulz F, Babinski M, Xu Y, Hu B, Chain PSG, Nayfach S, Kyrpides NC. 2024. Identification of mobile genetic elements with genomad. Nature Biotechnology. 42(8):1303-1312.

Carlier A, Fehr L, Pinto-Carbó M, Schäberle T, Reher R, Dessein S, König G, Eberl L. 2016. The genome analysis of *Candidatus* Burkholderia crenata reveals that secondary metabolism may be a key function of the ardisia crenata leaf nodule symbiosis. Environmental Microbiology. 18(8):2507-2522.

Carpenter SCD, Bogdanove AJ, Abbot B, Stajich JE, Uehling JK, Lovett B, Kasson MT, Carter ME. 2024. Prevalence and diversity of tal effector-like proteins in fungal endosymbiotic *Mycetohabitans* spp. Microbial Genomics. 10(6).

Carter ME, Carpenter SCD, Dubrow ZE, Sabol MR, Rinaldi FC, Lastovetsky OA, Mondo SJ, Pawlowska TE, Bogdanove AJ. 2020. A tal effector-like protein of an endofungal bacterium increases the stress tolerance and alters the transcriptome of the host. Proceedings of the National Academy of Sciences. 117(29):17122-17129.

Chaumeil P-A, Mussig AJ, Hugenholtz P, Parks DH. 2022. Gtdb-tk v2: Memory friendly classification with the genome taxonomy database. Bioinformatics. 38(23):5315-5316.

Cordaux R. 2009. Gene conversion maintains nonfunctional transposable elements in an obligate mutualistic endosymbiont. Molecular Biology and Evolution. 26(8):1679-1682.

Couvin D, Bernheim A, Toffano-Nioche C, Touchon M, Michalik J, Néron B, Rocha EPC, Vergnaud G, Gautheret D, Pourcel C. 2018. Crisprcasfinder, an update of crisrfinder, includes a portable version, enhanced performance and integrates search for cas proteins. Nucleic Acids Research. 46(W1):W246-W251.

Dale C, Young SA, Haydon DT, Welburn SC. 2001. The insect endosymbiont *Sodalis glossinidius* utilizes a type iii secretion system for cell invasion. Proceedings of the National Academy of Sciences. 98(4):1883-1888.

Delmont TO, Eren AM. 2018. Linking pangenomes and metagenomes: The *Prochlorococcus* metapangenome. PeerJ. 6:e4320.

Dewar AE, Hao C, Belcher LJ, Ghoul M, West SA. 2024. Bacterial lifestyle shapes pangenomes. Proceedings of the National Academy of Sciences. 121(21):e2320170121.

Dial DT, Weglarz KM, Aremu AO, Havill NP, Pearson TA, Burke GR, von Dohlen CD. 2022. Transitional genomes and nutritional role reversals identified for dual symbionts of adelgids (Aphidoidea: Adelgidae). Isme j. 16(3):642-654.

diCenzo GC, Finan TM. 2017. The divided bacterial genome: structure, function, and evolution. Microbiol Mol Biol Rev. 81(3).

Dolatabadi S, Scherlach K, Figge M, Hertweck C, Dijksterhuis J, Menken SB, de Hoog GS. 2016. Food preparation with mucoralean fungi: A potential biosafety issue? Fungal Biol. 120(3):393-401.

Eren AM, Kiefl E, Shaiber A, Veseli I, Miller SE, Schechter MS, Fink I, Pan JN, Yousef M, Fogarty EC et al. 2020. Community-led, integrated, reproducible multi-omics with anvi'o. Nature Microbiology. 6(1):3-6.

Estrada-De Los Santos P, Palmer M, Chávez-Ramírez B, Beukes C, Steenkamp E, Briscoe L, Khan N, Maluk M, Lafos M, Humm E et al. 2018. Whole genome analyses suggests that *Burkholderia* sensu lato contains two additional novel genera (*Mycetohabitans* gen. Nov., and *Trinickia* gen. Nov.): Implications for the evolution of diazotrophy and nodulation in the burkholderiaceae. Genes. 9(8):389.

Gilchrist CLM, Chooi Y-H. 2021. Clinker & clustermap.Js: Automatic generation of gene cluster comparison figures. Bioinformatics. 37(16):2473-2475.

Goodhead I, Blow F, Brownridge P, Hughes M, Kenny J, Krishna R, McLean L, Pongchaikul P, Beynon R, Darby AC. 2020. Large-scale and significant expression from pseudogenes in *Sodalis glossinidius* – a facultative bacterial endosymbiont. Microbial Genomics. 6(1).

Grujcic V, Mehrshad M, Vigil-Stenman T, Lundin D, Foster RA. 2025. The path to dependence: Stepwise genome evolution from a facultative symbiont to an endosymbiont in the N_2-fixing diatom-*Richelia* symbioses. bioRxiv.2025.2003.2025.645212.

Harrison PW, Lower RPJ, Kim NKD, Young JPW. 2010. Introducing the bacterial 'chromid': Not a chromosome, not a plasmid. Trends in Microbiology. 18(4):141-148.

Hendry TA, Freed LL, Fader D, Fenolio D, Sutton TT, Lopez JV. 2018. Ongoing transposon-mediated genome reduction in the luminous bacterial symbionts of deep-sea ceratioid anglerfishes. mBio. 9(3):10.1128/mbio.01033-01018.

Heuer H, Krsek M, Baker P, Smalla K, Wellington EM. 1997. Analysis of actinomycete communities by specific amplification of genes encoding 16S rRNA and gel-electrophoretic separation in denaturing gradients. Appl Environ Microbiol. 63(8):3233-3241.

Hyatt D, Chen G-L, Locascio PF, Land ML, Larimer FW, Hauser LJ. 2010. Prodigal: Prokaryotic gene recognition and translation initiation site identification. BMC Bioinformatics. 11(1):119.

Jain C, Rodriguez-R LM, Phillippy AM, Konstantinidis KT, Aluru S. 2018. High throughput ANI analysis of 90k prokaryotic genomes reveals clear species boundaries. Nature Communications. 9(1):5114.

Julian AT, Pombert JF. 2024. Syny: A pipeline to investigate and visualize collinearity between genomes. bioRxiv.

Keeling PJ, McCutcheon JP. 2017. Endosymbiosis: The feeling is not mutual. Journal of Theoretical Biology. 434:75-79.

Kolmogorov M, Yuan J, Lin Y, Pevzner PA. 2019. Assembly of long, error-prone reads using repeat graphs. Nature Biotechnology. 37(5):540-546.

Konstantinidis KT. 2023. Sequence-discrete species for prokaryotes and other microbes: A historical perspective and pending issues. mLife. 2(4):341-349.

Kryazhimskiy S, Plotkin JB. 2008. The population genetics of dN/ds. PLOS Genetics. 4(12):e1000304.

Kumar S, Stecher G, Li M, Knyaz C, Tamura K. 2018. Mega x: Molecular evolutionary genetics analysis across computing platforms. Mol Biol Evol. 35(6):1547-1549.

Lackner G, Möbius N, Scherlach K, Partida-Martinez Laila P, Winkler R, Schmitt I, Hertweck C. 2009. Global distribution and evolution of a toxinogenic *Burkholderia-Rhizopu*s symbiosis. Applied and Environmental Microbiology. 75(9):2982-2986.

Lackner G, Moebius N, Partida-Martinez LP, Boland S, Hertweck C. 2011. Evolution of an endofungal lifestyle: Deductions from the *Burkholderia rhizoxinica* genome. BMC Genomics. 12(1):210.

Lan Y, Sun J, Chen C, Wang H, Xiao Y, Perez M, Yang Y, Kwan YH, Sun Y, Zhou Y et al. 2022. Endosymbiont population genomics sheds light on transmission mode, partner specificity, and stability of the scaly-foot snail holobiont. The ISME Journal. 16(9):2132-2143.

Li H. 2016. Minimap and miniasm: Fast mapping and *de novo* assembly for noisy long sequences. Bioinformatics. 32(14):2103-2110.

Lind AE, Lewis WH, Spang A, Guy L, Embley TM, Ettema TJG. 2018. Genomes of two archaeal endosymbionts show convergent adaptations to an intracellular lifestyle. The ISME Journal. 12(11):2655-2667.

Mahmood S, Nováková E, Martinů J, Sychra O, Hypša V. 2023. Supergroup F *Wolbachia* with extremely reduced genome: Transition to obligate insect symbionts. Microbiome. 11(1):22.

McCutcheon JP, Moran NA. 2012. Extreme genome reduction in symbiotic bacteria. Nature Reviews Microbiology. 10(1):13-26.

Mondo SJ, Lastovetsky OA, Gaspar ML, Schwardt NH, Barber CC, Riley R, Sun H, Grigoriev IV, Pawlowska TE. 2017. Bacterial endosymbionts influence host sexuality and reveal reproductive genes of early divergent fungi. Nature Communications. 8(1):1843.

Moses D, Carter M. 2025. A plant health view on endohyphal bacteria and their fungal hosts. Phytobiomes Journal. 0(0):PBIOMES-12-24-0117-MRVW.

Mullins AJ, Mahenthiralingam E. 2021. The hidden genomic diversity, specialized metabolite capacity, and revised taxonomy of *Burkholderia* sensu lato. Frontiers in Microbiology. Volume 12 - 2021.

Naumann M, Schüßler A, Bonfante P. 2010. The obligate endobacteria of arbuscular mycorrhizal fungi are ancient heritable components related to the mollicutes. The ISME Journal. 4(7):862-871.

Nayfach S, Camargo AP, Schulz F, Eloe-Fadrosh E, Roux S, Kyrpides NC. 2021. CheckV assesses the quality and completeness of metagenome-assembled viral genomes. Nature Biotechnology. 39(5):578-585.

Niehs SP, Dose B, Richter S, Pidot SJ, Dahse HM, Stinear TP, Hertweck C. 2020. Mining symbionts of a spider-transmitted fungus illuminates uncharted biosynthetic pathways to cytotoxic benzolactones. Angew Chem Int Ed Engl. 59(20):7766-7771.

Niehs SP, Scherlach K, Dose B, Uzum Z, Stinear TP, Pidot SJ, Hertweck C. 2022. A highly conserved gene locus in endofungal bacteria codes for the biosynthesis of symbiosis-specific cyclopeptides. PNAS Nexus. 1(4).

Paradis E, Claude J, Strimmer K. 2004. Ape: Analyses of phylogenetics and evolution in r language. Bioinformatics. 20(2):289-290.

Parks DH, Chuvochina M, Waite DW, Rinke C, Skarshewski A, Chaumeil P-A, Hugenholtz P. 2018. A standardized bacterial taxonomy based on genome phylogeny substantially revises the tree of life. Nature Biotechnology. 36(10):996-1004.

Parks DH, Imelfort M, Skennerton CT, Hugenholtz P, Tyson GW. 2015. CheckM: Assessing the quality of microbial genomes recovered from isolates, single cells, and metagenomes. Genome Res. 25(7):1043-1055.

Partida-Martinez LP, Hertweck C. 2005. Pathogenic fungus harbours endosymbiotic bacteria for toxin production. Nature. 437(7060):884-888.

Partida-Martinez LP, Hertweck C. 2007. A gene cluster encoding rhizoxin biosynthesis in "*Burkholderia rhizoxina*", the bacterial endosymbiont of the fungus rhizopus microsporus. 8:41–45.

Partida-Martinez LP, Monajembashi S, Greulich K-O, Hertweck C. 2007. Endosymbiont-dependent host reproduction maintains bacterial-fungal mutualism. Current Biology. 17(9):773-777.

Pawlowska TE. 2024. Symbioses between fungi and bacteria: From mechanisms to impacts on biodiversity. Current Opinion in Microbiology. 80:102496.

Porter J, Sullivan W. 2023. The cellular lives of *Wolbachia*. Nature Reviews Microbiology. 21(11):750-766.

Pratama AA, Chaib De Mares M, Van Elsas JD. 2018. Evolutionary history of bacteriophages in the genus *Paraburkholderia*. Frontiers in Microbiology. 9.

Robinson AJ, House GL, Morales DP, Kelliher JM, Gallegos-Graves LV, LeBrun ES, Davenport KW, Palmieri F, Lohberger A, Bregnard D et al. 2021. Widespread bacterial diversity within the bacteriome of fungi. Communications Biology. 4(1):1168.

Seo Y-S, Lim JY, Park J, Kim S, Lee H-H, Cheong H, Kim S-M, Moon JS, Hwang I. 2015. Comparative genome analysis of rice-pathogenic *Burkholderia* provides insight into capacity to adapt to different environments and hosts. BMC Genomics. 16(1):349.

Simão FA, Waterhouse RM, Ioannidis P, Kriventseva EV, Zdobnov EM. 2015. BUSCO: Assessing genome assembly and annotation completeness with single-copy orthologs. Bioinformatics. 31(19):3210-3212.

Siozios S, Nadal-Jimenez P, Azagi T, Sprong H, Frost CL, Parratt SR, Taylor G, Brettell L, Liew KC, Croft L et al. 2024. Genome dynamics across the evolutionary transition to endosymbiosis. Current Biology. 34(24):5659-5670.e5657.

Steffan BN, Venkatesh N, Keller NP. 2020. Let's get physical: Bacterial-fungal interactions and their consequences in agriculture and health. J Fungi (Basel). 6(4).

Sun Y, Wang M, Cao L, Seim I, Zhou L, Chen J, Wang H, Zhong Z, Chen H, Fu L et al. 2023. Mosaic environment-driven evolution of the deep-sea mussel *Gigantidas platifrons* bacterial endosymbiont. Microbiome. 11(1):253.

Szabó G, Schulz F, Manzano-Marín A, Toenshoff ER, Horn M. 2021. Evolutionarily recent dual obligatory symbiosis among adelgids indicates a transition between fungus- and insect-associated lifestyles. The ISME Journal. 16(1):247-256.

Szabó G, Schulz F, Manzano-Marín A, Toenshoff ER, Horn M. 2022. Evolutionarily recent dual obligatory symbiosis among adelgids indicates a transition between fungus- and insect-associated lifestyles. The ISME Journal. 16(1):247-256.

Tatusova T, DiCuccio M, Badretdin A, Chetvernin V, Nawrocki EP, Zaslavsky L, Lomsadze A, Pruitt KD, Borodovsky M, Ostell J. 2016. Ncbi prokaryotic genome annotation pipeline. Nucleic Acids Res. 44(14):6614-6624.

Tettelin H, Riley D, Cattuto C, Medini D. 2008. Comparative genomics: The bacterial pan-genome. Current Opinion in Microbiology. 11(5):472-477.

Thompson JD, Higgins DG, Gibson TJ. 1994. Clustal w: Improving the sensitivity of progressive multiple sequence alignment through sequence weighting, position-specific gap penalties and weight matrix choice. Nucleic Acids Res. 22(22):4673-4680.

Turenne CY, Sanche SE, Hoban DJ, Karlowsky JA, Kabani AM. 1999. Rapid identification of fungi by using the its2 genetic region and an automated fluorescent capillary electrophoresis system. J Clin Microbiol. 37(6):1846-1851.

Uehling J, Gryganskyi A, Hameed K, Tschaplinski T, Misztal PK, Wu S, Desirò A, Vande Pol N, Du Z, Zienkiewicz A et al. 2017. Comparative genomics of *Mortierella elongata* and its bacterial endosymbiont *Mycoavidus cysteinexigens*. Environmental Microbiology. 19(8):2964-2983.

Vancaester E, Blaxter M. 2023. Phylogenomic analysis of *wolbachia* genomes from the darwin tree of life biodiversity genomics project. PLOS Biology. 21(1):e3001972.

Vigil-Stenman T, Larsson J, Nylander JAA, Bergman B. 2015. Local hopping mobile DNA implicated in pseudogene formation and reductive evolution in an obligate cyanobacteria-plant symbiosis. BMC Genomics. 16(1):193.

Wang X, Xiong X, Cao W, Zhang C, Werren JH, Wang X. 2020. Phylogenomic analysis of *Wolbachia* strains reveals patterns of genome evolution and recombination. Genome Biol Evol. 12(12):2508-2520.

Wang X, Zhou H, Chen H, Jing X, Zheng W, Li R, Sun T, Liu J, Fu J, Huo L et al. 2018. Discovery of recombinases enables genome mining of cryptic biosynthetic gene clusters in Burkholderiales species. Proceedings of the National Academy of Sciences. 115(18):E4255-E4263.

Wernegreen JJ. 2015. Endosymbiont evolution: Predictions from theory and surprises from genomes. Ann N Y Acad Sci. 1360(1):16-35.

Westra ER, Levin BR. 2020. It is unclear how important CRISPR-Cas systems are for protecting natural populations of bacteria against infections by mobile genetic elements. Proceedings of the National Academy of Sciences. 117(45):27777-27785.

Xie Z, Tang H. 2017. Isescan: Automated identification of insertion sequence elements in prokaryotic genomes. Bioinformatics. 33(21):3340-3347.

Yu G, Smith DK, Zhu H, Guan Y, Lam TT-Y. 2017. ggtree: An R package for visualization and annotation of phylogenetic trees with their covariates and other associated data. Methods in Ecology and Evolution. 8(1):28-36.